

# Hierarchical Windowed Graph Attention Network and a Large Scale Dataset for Isolated Indian Sign Language Recognition

Suvajit Patra  
RKMVERI  
Belur, India

suvajit.patra.cs20@gm.rkmvu.ac.in

Arkadip Maitra  
RKMVERI  
Belur, India

arkadipmaitra@gmail.com

Megha Tiwari  
FDMSE, RKMVERI  
Coimbatore, India

mghgpt84@gmail.com

K. Kumaran  
FDMSE, RKMVERI  
Coimbatore, India

k6kumaran@gmail.com

Swathy Prabhu  
RKMVC  
Chennai, India

swathyprabhu@gmail.com

Swami Punyeshwarananda  
RKMVERI  
Belur, India

punyeshwarananda@gm.rkmvu.ac.in

Soumitra Samanta  
RKMVERI  
Belur, India

soumitra.samanta@gm.rkmvu.ac.in

## Abstract

*Automatic Sign Language (SL) recognition is an important task in the computer vision community. To build a robust SL recognition system, we need a considerable amount of data which is lacking particularly in Indian sign language (ISL). In this paper, we propose a large-scale isolated ISL dataset and a novel SL recognition model based on skeleton graph structure. The dataset covers 2,002 daily used common words in the deaf community recorded by 20 (10 male and 10 female) deaf adult signers (contains 40033 videos). We propose a SL recognition model namely Hierarchical Windowed Graph Attention Network (HWGAT) by utilizing the human upper body skeleton graph structure. The HWGAT tries to capture distinctive motions by giving attention to different body parts induced by the human skeleton graph structure. The utility of the proposed dataset and the usefulness of our model are evaluated through extensive experiments. We pre-trained the proposed model on the proposed dataset and fine-tuned it across different sign language datasets further boosting the performance of 1.10, 0.46, 0.78, and 6.84 percentage points on INCLUDE [46], LSA64 [41], AUTSL [45] and WLASL [25] respectively compared to the existing state-of-the-art skeleton-based models. The proposed dataset and the model implementation code will be available at <https://cs.rkmvu.ac.in/~isl>.*

## 1. Introduction

Sign Language (SL) is a natural language with unique grammatical and linguistic characteristics. The deaf and mute community developed this to communicate with each other and socialize. As a visual language, SL conveys information by adopting the articulation of human body parts with manual characteristics such as hand shapes, body pose, and the interaction of hands with different body parts, together with non-manual characteristics such as facial expression and head movement [1,42].

According to the World Health Organization (WHO), around 5% (430 million) people around the world suffer from hearing loss [11]. To bridge the communication gap between signers (people with sign language as their primary communication medium) and non-signers (people with spoken language proficiency rather than sign language) the automatic SL recognition field has emerged and gained popularity among computer vision and machine learning researchers [26, 48, 54]. This task contains 2 subtasks, 1) *isolated SL* recognition - which maps every sign video to the corresponding gloss, and 2) *continuous SL* recognition - which maps every sign video to a sequence of glosses. Here our focus is on isolated sign language recognition. Similar to any recognition task, to build a good SL recognition model, we need a sufficient amount of data to get a considerable inference. Researchers have proposed different datasets for different SL recognition tasks, for example, MS-ASL [20], WLASL [25], ASLLVD [4] for the isolated

American SL recognition task. For the British SL recognition task, there are datasets like BOB-SL [3], and BSL-Dict [31]. Also, there are other datasets [41, 45, 54] for different sign languages.

The Indo-Pakistani sign language is the most used sign language in the world and about 15 million deaf signers use this in their daily communications<sup>1</sup>. In comparison to other sign languages Indian Sign Language (ISL) contains a higher number of composite signs (signs made up of two or more glosses). For example, the word *Wife* sign consists of the *Female* and *Marriage* signs [46]. These factors make ISL recognition task both important and unique. For automatic ISL recognition task, there are not many resource-rich publicly available datasets in the literature. Some limited attempts have been made with INCLUDE [46] and CISLR [19] containing a limited number of sign videos per word. This provides the impetus for creating a resource-rich isolated ISL dataset. We propose a resource-rich isolated ISL dataset containing 40033 sign video with 20 videos per sign word (contains 2002 words).

In general, the sign language recognition task is a sub-domain of human action recognition from video data and it inherits all the challenges such as blurred boundaries between classes, occlusion of body parts, human appearance, recording environments and recording settings [34]. Also, sign language glosses contain very subtle spatial and temporal differentiable features, which introduces another level of complexity. This makes the sign language (particularly ISL) recognition task more challenging than action recognition and state-of-the-art action recognition models fall short in SL recognition tasks.

To model the SL recognition task we consider the signer’s skeleton joint points from sign videos and represent that as a spatio-temporal skeleton graph structure. We learn the graph structure in natural language processing settings. Usually, spoken language is represented by a 1-dimensional sequence of words with well-defined syntax and semantics, and its structure is successfully modeled by the attention mechanism [49]. However, the skeleton graph extracted from sign videos is a 3-dimensional data with complex spatio-temporal context, and it is non-trivial to analogically define visual word or unit with clarified semantics. Existing graph based approaches and normal baseline approaches face difficulty in recognition from this spatio-temporal skeleton data. To tackle these issues, we propose a novel Hierarchical Windowed Graph Attention Network (HWGAT). The proposed model conserves the skeleton graph structure and attention mechanism along with input partitioning so that specific sign expressions such as expressive hand movements can be processed without unwanted influence from the other body parts. Through extensive experiments, we justify different design decisions in

the HWGAT model. We evaluate the HWGAT model on the proposed dataset and other state-of-the-art datasets and report comparative results. In this paper, our main contributions are as follows:

1. We propose a large-scale isolated ISL dataset consisting of over 40,000 videos containing a rich and large vocabulary of 2,002 daily used words in ISL conversations. It contains unique characteristics like 20 signers, gender-balanced and signer-independent sets (no intersection of signers in training, validation, and testing sets). It also contains sign word analysis and their categorizations into different groups based on the number of glosses (e.g. atomic, composite).
2. We propose a novel windowed graph attention-based model specifically developed for sign language recognition on skeleton graphs.
3. We publish our automated recording and annotations pipeline to ease such data collection process in any sign language.

The rest of the paper is organized as follows: Section 2 provides an overview of the existing sign language datasets and recognition techniques. The characteristics of the proposed dataset are described in Section 3. Section 4 presents the working mechanism of our proposed framework. The experiment, results and analysis are given in Section 5 followed by conclusion in Section 6.

## 2. Related Works

In the literature, there are limited numbers of datasets on Indian sign language (ISL) recognition tasks. In this section, first, we review the existing ISL datasets followed by some state-of-the-art other sign language datasets for different languages. Then review some state-of-the-art sign language recognition models.

For ISL recognition, the initial datasets were primarily consisting of a few image samples or a very limited number of sign videos. To the best of our knowledge, the first ISL dataset proposed by Rekha *et al.*, consists of 290 images for 26 alphabets [39]. One early dataset containing 600 videos corresponding to 22 sign word classes [32] and another dataset with 800 sign videos for 80 signs [22] suffer from either a limited vocabulary size or a low number of samples per class. These datasets are not sufficient for robust real-world applications. The largest available ISL dataset namely CISLR, containing 7050 videos with over 4765 sign words [19], suffers from less number of per-class samples, making it inconsistent for real-world sign language recognition tasks and is viable only for one-shot learning tasks. In literature, the largest standard isolated ISL dataset INCLUDE [46] has a collection of 263 signs, recorded with 7

<sup>1</sup><https://www.ethnologue.com/>

Table 1. Comparison of FDMSE-ISL dataset with the state-of-the-art isolated sign language datasets.

Dataset	Language	# Signs	# Sign video (avg. per sign)	# Signers	Source	# Hours
ASLLVD [4]	American (ASL)	2,742	9K (3)	6	lab	4
ASL-LEX 2.0 [43]	American (ASL)	2,723	2723(1)	-	lexicons, lab, web	-
MSASL [20]	American (ASL)	1,000	25K(25)	222	lexicons, web	25
WLASL [25]	American (ASL)	2,000	21K (11)	119	lexicons, web	14
LSA64 [41]	Argentinian	64	3K (47)	10	-	1.9
BSLDict [31]	British (BSL)	9,283	14K (1)	148	lexicons	9
DEVISIGN-L [50]	Chinese (CSL)	2,000	24K (12)	8	lab	13-33
SLR500 [54]	Chinese (CSL)	500	125K (250)	50	lab	69-139
GSL [1]	Greek (GSL)	310	40K()	7	-	6.4
SMILE [12]	Swiss German (DSGS)	100	9K (90)	30	lab	-
BosphorusSion22k [33]	Turkish (TSL)	744	23K (30)	6	lab	19
AUTSL [45]	Turkish (TSL)	226	38K (170)	43	lab	21
INCLUDE [46]	Indian (ISL)	263	4K (16)	7	lab	3
CISLR [19]	Indian (ISL)	4765	7K (1)	71	web	3
<b>FDMSE-ISL</b>	Indian (ISL)	2,002	40K (20)	20	lab	36

signers (students) in a classroom setting with a static background, and contains a total of 4,287 videos. Even this dataset contains very limited vocabulary compared to the vocabulary size used by ISL signers in their daily communications.

For other sign languages, there exists a number of large-scale sign language datasets shown in Table 1. Athitsos *et al.* [4] proposed an isolated American Sign Language (ASL) dataset called ASLLVD, consisting of 9,800 video samples of 3,300 sign words, recorded with 1-6 native signers. Another isolated ASL dataset called MS-ASL [20] proposed by Jose and Koller covering 25,000 videos of 1,000 sign words with 222 signers. To make the dataset challenging they recorded the videos in unconstrained real-life conditions. In the recent past, Li *et al.* [25] proposed a word-level ASL dataset (WLASL) with a total of 21,083 video samples of 2,000 signs with 119 signers. The videos are collected from different web sources. Momeni *et al.* [31] proposed a British Sign Language (BSL) dataset known as BSLDict which contains a large vocabulary of size 9,283 and is created with 148 signers. There is a sign language dataset for Turkish Sign Language (TSL) proposed by Sincan and Keles [45] called AUTSL, which contains 38,336 video samples of 226 signs performed by 43 different signers. The videos are recorded in both indoor and outdoor environments. This dataset has color, depth, and skeleton modalities. Some other isolated SL datasets include Chinese Sign Language (CSL) SLR500 [54] contains 125,000 videos spanning over 500 signs. The SMILE [12] dataset is the isolated Swiss German Sign Language (DSGS) dataset containing 100 signs with 9,000 videos.

To the best of our knowledge, in terms of video count, the proposed dataset contains the maximum number of videos compared to the other isolated sign language datasets

shown in Table 1, except the SLR500 dataset. However, the SLR500 dataset only contains a vocabulary of 500 signs, and each sign is repeated five times by each signer. Regarding vocabulary size, the sign language dictionaries ASLLVD [4], ASL-LEX 2.0 [43], WLASL [25], and BSLDict [31] have demonstrated comparable or greater coverage of signs. However, they have fewer videos per sign as shown in Table 1.

In general, researchers try to tackle the SL recognition task as a pattern recognition task. It contains two subtasks namely 1) *feature extraction*: where each sign video is represented as a fixed dimensional feature vector and 2) *recognition*: where the represented videos are classified using a standard classifier. For feature extraction, initially researchers [18,26,33,48,54] have tried some hand-crafted features like Histogram of Oriented Gradient (HOG) [9], Scale Invariant Feature Transform (SIFT) [28], Optical Flow [14]. They classify each sign using standard classifiers like HMM [24,35], SVM [37], and Random Forest [2].

After the prevalence of deep learning methods due to their performance overhead over traditional methods, researchers are leveraging advanced feature extraction and classification techniques using deep learning methods. Particularly in the domain of SL recognition, deep learning-based methods are broadly classified into two types. The first approach involves extracting features from each raw RGB video using various methods such as two-dimensional (2D) CNN [23,38], 3D CNN [15,25], and CNN models with Bi-LSTM decoder [10]. These features are classified into glosses using *one* or more fully connected layers. In addition to RGB videos Jiang *et al.* [17] utilized depth, skeleton, and motion information to enhance the recognition of Turkish sign language. Further advancements by

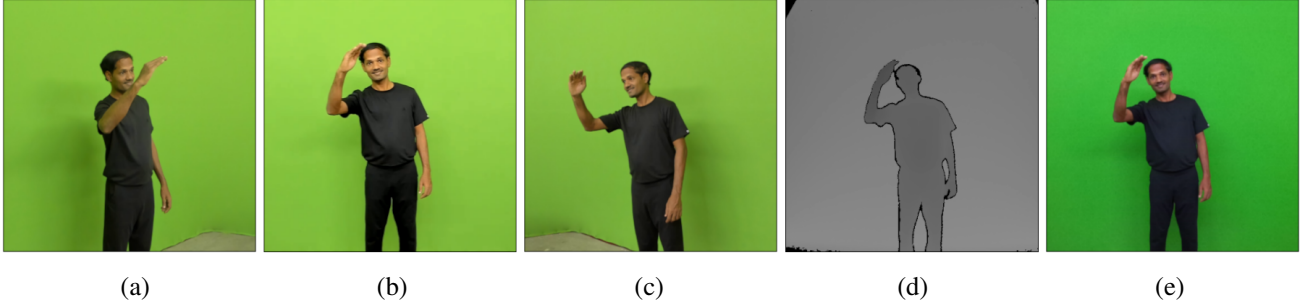


Figure 1. Sample frame of the sign "Hello" in all the *five* modalities ((a) left (60fps), (b) front (60fps), (c) right (60fps), (d) Azure Kinect DK depth (30fps) and (e) Azure Kinect DK RGB (30fps)) available in the dataset.

Zuo *et al.* [56] have integrated natural language glosses during the training process, resulting in state-of-the-art performance across multiple SL datasets. Despite these advancements, RGB-based methods are computationally expensive, and their slow classification time poses limitations for real-time sign language recognition.

In the second type of approach, researchers detect the skeleton keypoints of the signer using the state-of-the-art human pose estimation methods like MediaPipe [29], OpenPose [7], MMPose [8], Yolo-pose [30] etc. The extracted sequential pose data is processed using various sequential data models including GRU [25], LSTM [21, 26], and different variants of Transformers [5, 6, 44] for SL recognition task. Subsequently, researchers have represented sequential pose data as skeleton graphs and employed Graph Convolutional Networks (GCNs) due to their ability to capture contextual information from graphical data effectively. Yan *et al.* [52] first introduced a GCN on the sequential human keypoints data as a spatio-temporal graph using natural human joint connectivity and called it ST-GCN. Jiang *et al.* adopted this model for Turkish sign language recognition, by cascading spatial, temporal and channel importance to the GCN block and called it SL-GCN [17]. The ST-GCN and SL-GCN models were applied to the Indian sign language recognition task on the INCLUDE [44] dataset. During inference, these models perform convolution operations and give static weights to the connected neighbours of a node irrespective of their feature representations.

Here, we propose a graph attention-based network named Hierarchical Windowed Graph Attention Network (HWGAT), where we use an attention mechanism which takes the node features into consideration to generate dynamic attention weights instead of using static kernel weights. This resulted in better performance compared to skeleton-based models across multiple SL datasets.

### 3. Proposed Dataset

This paper presents a large-scale isolated sign language dataset for SL recognition tasks in general and in particular for Indian sign language recognition tasks. In the creation of this dataset, we followed the FDMSE's [16] dictionary which was published in consultations with sign experts throughout India. We carefully considered 2,002 common words used in daily communications among the deaf community from that dictionary. The words are categorised into 57 groups *i.e.* 'family relations', 'behaviour norms', 'body parts', 'household articles' etc. We further studied all the signs and grouped them into two categories, namely, atomic signs or glosses (that cannot be decomposed into other meaningful signs (eg. *marriage*)) and composite signs (can be decomposed into atomic signs or glosses (eg. *wife*  $\rightarrow$  *female* + *marriage*)).

We collected the dataset with the help of 20 native ISL signers (deaf) from the southern part of India. To ensure that the dataset is gender unbiased, we have considered 10 male and 10 female subjects. For data collection setup, we used a static background with a green screen to facilitate the segmentation process.

We have recorded the videos from four different viewing positions: two frontal, approximately 30° left, and 30° right with respect to the frontal view of the subject. *Three Logitech BRIO* 60 fps cameras were used for recording the videos in landscape mode with a frame size of 1920 × 1080. Furthermore, to capture the depth information *one Azure Kinect DK* camera is used at the front position. By keeping single-view real-world SL recognition applications in mind, this work is focused on the frontal RGB camera data only. But all the 5 modalities (*four*-RGB and *one*-depth modalities) recorded will be publicly available (<https://cs.rkmvu.ac.in/~isl>) and can be used for research purposes only. Furthermore, apart from the frontal RGB modality, the other multiview modalities can also be used for tasks such as keypoints correction, pose estimation, 3D-model generation, and general gesture recognition. The

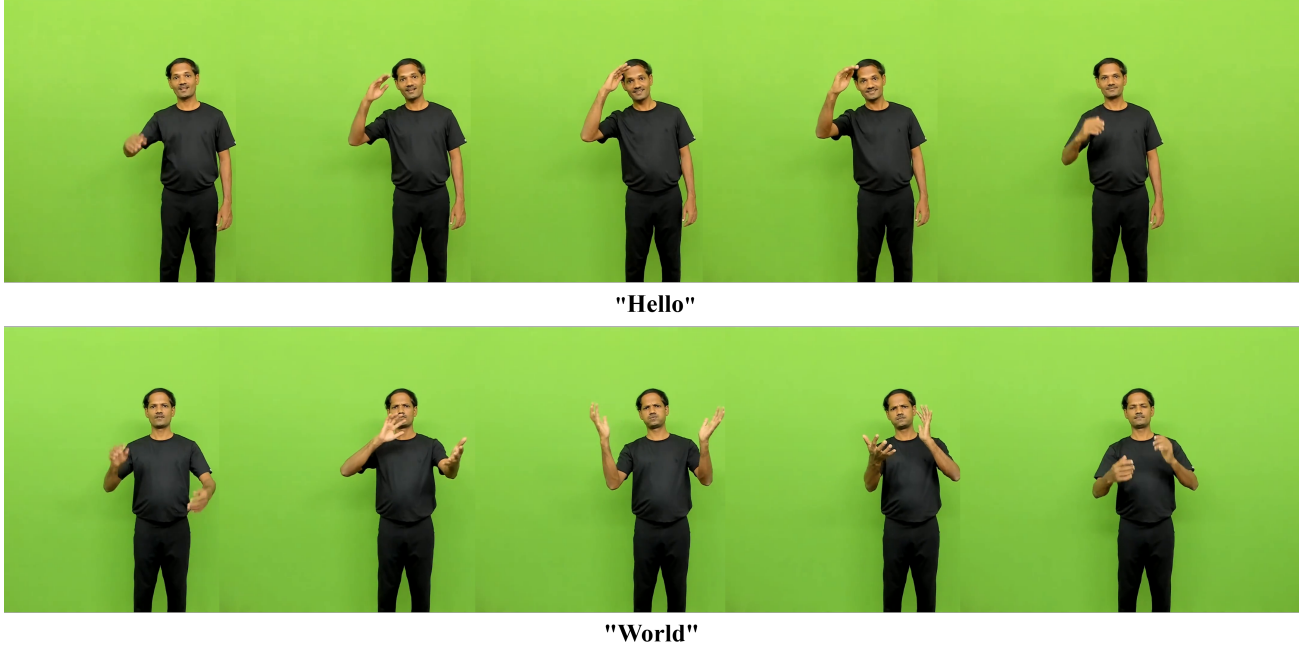


Figure 2. Sample frames from the signs "Hello" and "World".

videos were recorded in the lab settings with required ethical clearance and a standard dress code (matt black) under the supervision of certified ISL experts.

We built a custom tool named Word Viewer and Timeline Manager (WVTM) to manage and automatically annotate the large corpus of videos. During recording, the operator uses the WVTM tool first to show a sign word to the subject with a prompt and then register the event (session start, start recording for a word, stop recording for a word, session end etc.) timestamps in a log file. After recording all the sessions, a Python script is used to automatically split the videos and annotate them using the log files generated during the recording. The complete annotation and recording pipeline will be publicly available (<https://cs.rkmvu.ac.in/~isl>) to simplify the dataset collection process for any sign language.

In total, the dataset from the frontal RGB camera contains 40,033 videos across 2,002 words. The total duration of the dataset is around 36.2 hours with 7.8 Million frames. The average duration of the sign videos is around 3.25 seconds. We crop the original videos to  $1200 \times 950$  resolution keeping the signer at the centre. Table 2 summarizes the statistics of the dataset. For each sign word, there are *five* different modalities (frontal both 60 fps and 30 fps, two side views at  $\approx \pm 30$  degrees 60 fps and depth information) from *four* viewing positions. For the experiments in this paper we used 40,033 videos from the frontal 60 fps RGB camera. Figure 1 shows the sample frames from each camera view and Figure 2 shows some frames of two signs 'Hello'

and 'World'.

The proposed dataset excels in several aspects from the existing ISL dataset INCLUDE [46]. For example, the proposed dataset contains around a 7.6 times higher number of signs and a 9.3 times higher number of videos. Furthermore, our dataset has more qualitative diversity in terms of age, height, and skin tone. For instance, the INCLUDE [46] dataset was recorded with young students of similar age, whereas our signers' approximate age ranged between 28 and 55, and height between 4.5 and 6 feet. While our dataset is multimodal and multicamera, the INCLUDE dataset was recorded with a single camera.

To evaluate the proposed model on the proposed dataset, we divide the dataset in train, validation, and test partitions into 5 : 1 : 4 ratios on randomly chosen subjects (signers) so that the training set, validation set and test set have no intersection of signers. In total, there are 10 subjects in training (5 male, 5 female), 2 for validation (1 male, 1 female) and 8 for testing (4 male, 4 female). Finally, we used 20,016, 4,003, and 16,014 videos for training, validation, and testing respectively.

#### 4. Proposed Approach

The objective of this work is to create a sign language recognition system that works on extracted keypoints from any sign video. According to ISL experts, the influence of different body parts on any particular sign is essential, especially hands. The body keypoints and the edges connecting these keypoints form a graph structure. Classifi-

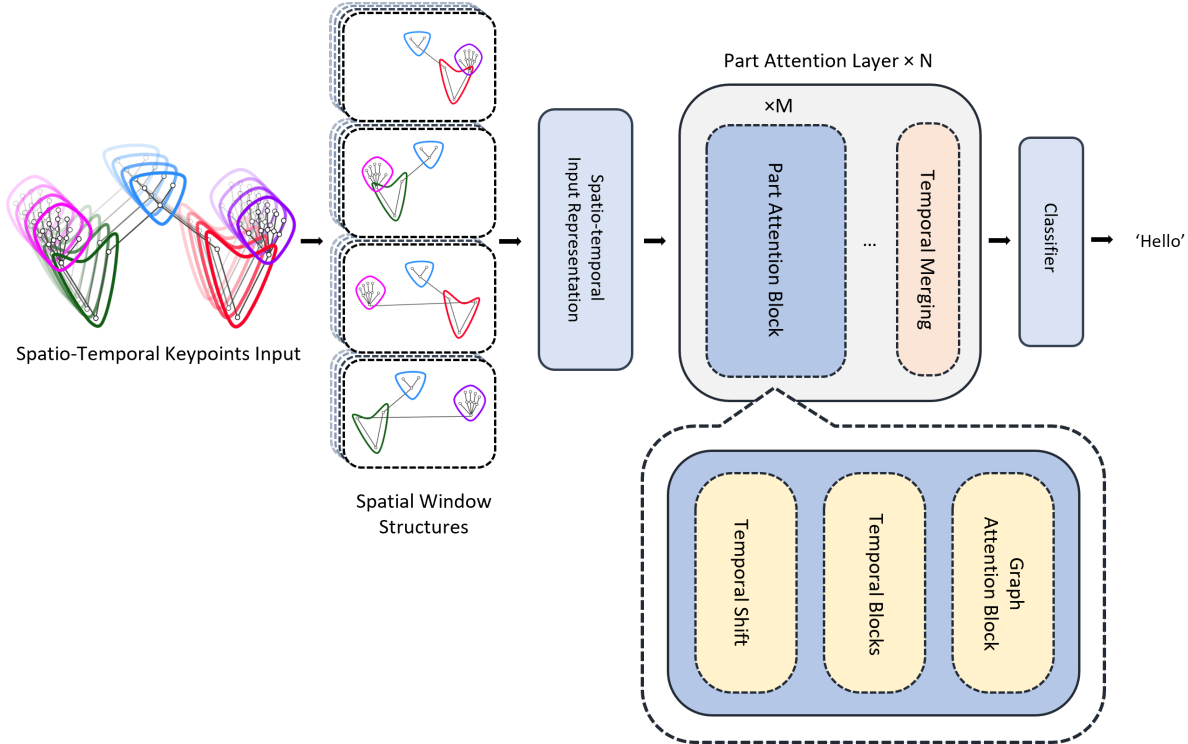


Figure 3. The proposed Hierarchical Windowed Graph Attention Network (HWGAT) takes the spatio-temporal graph structure as input and divides this graph into multiple spatial windows based on distinct body parts as represented in Figure 4. Next, multiple part attention layers are applied on this windowed graph structure to extract features and a fully connected layer is used to get the sign word.

Table 2. Summary of the FDMSE-ISL dataset.

Parameters	Values
Words	2002
Videos	40033
Groups	57
Avg Videos per Class	$\approx 20$
Avg Video Length	3.25s
Min Video Length	1.5s
Max Video Length	9.5s
Frame Rate	60 fps, 30 fps
Resolution	$1200 \times 950, 512 \times 512$
Modalities	4 RGB, 1 depth

cation of these graph structures are generally modeled by Graph Convolutional Networks (GCN) [17, 52]. In general, GCN models are homogenous to CNNs where the kernel in CNN is similar to the learned adjacency matrix in GCN. But, even after the training process, the elements of the adjacency matrix are static. We propose the Hierarchical Windowed Graph Attention Network (HWGAT) where we use the attention mechanism which takes the node features into consideration to generate dynamic attention weight instead of fixed kernel weight. Therefore giving importance

to the neighbourhood nodes based on their similarity during information sharing. Also to incorporate the importance of body parts for any sign word recognition our attention mechanism is designed to be restricted according to the spatio-temporal skeleton graph. An overview of the proposed HWGAT is presented in Figure 3. This model consists of two major parts namely spatio-temporal input representation and part attention layer. We represent the input graph structure as follows:

#### 4.1. Spatio-temporal Input Representation:

The spatio-temporal input representation consists of 2 parts: *skeleton graph representation and spatial window substructures*. We select 27 keypoints from each frame of a sign video, encompassing 3 facial keypoints (nose, 2 eyes), 2 shoulders, 2 elbows, and 10 keypoints from each hand to represent the spatial skeleton graph input for our model as shown in Figure 5. These keypoints are selected based on recommendations from SL experts and inspired by [18, 44]. The keypoint graph generated from an entire video consists of  $F$  frames and each frame contains  $K$  keypoints. Each keypoint is represented as a 2D vector with  $x$  and  $y$  coordinates, forming nodes in this generated spatio-temporal keypoint graph. The edge set  $E(G)$  for the entire graph is constructed as follows:

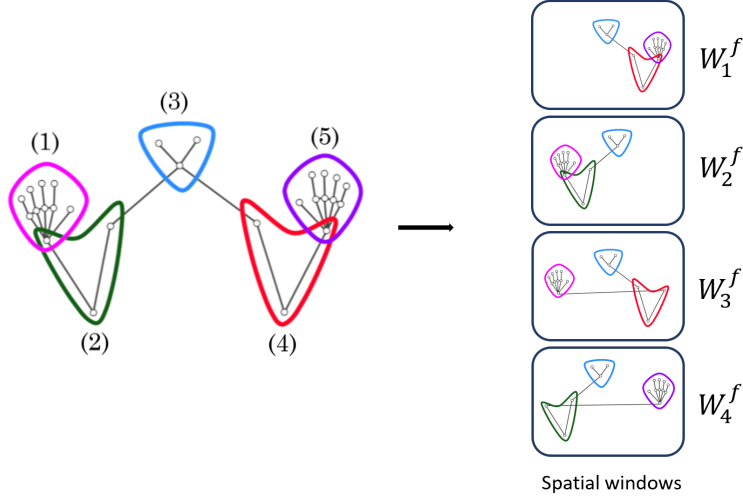


Figure 4. Grouping of spatial keypoints into the 5 body parts. The part marked as 1 contains the selected right-hand keypoints, the part marked as 2 has the right arm keypoints, the part marked as 3 has the selected face keypoints, the part marked as 4 is the left-arm and 5 marks the left-hand keypoints respectively. These part combinations are used to create the 4 spatial windows.



Figure 5. Visual representation of 27 keypoints used as input (10 per hands and 7 pose points with connections).

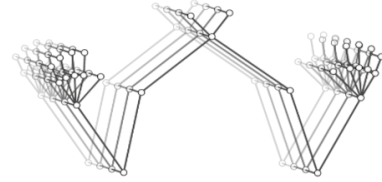


Figure 6. The spatio-temporal skeleton graph obtained from a sign language video.

$$E(G) = \begin{cases} e_{i,j}^t = 1, & \text{if } v_i, v_j \text{ are connected spatially} \\ e_i^{t,t+1} = 1, & \text{temporal connection} \\ e_i^t = 0, & \text{otherwise} \end{cases} \quad (1)$$

where,  $t \in \{1, 2, \dots, (F-1)\}$  denotes the frame index,  $v$  is a node with indices  $i, j \in \{1, 2, \dots, K\}$  and  $e$  represents a particular edge in the graph. Figure 6 illustrates the visual representation of the whole spatio-temporal skeleton structure of a sign video. This spatio-temporal skeleton structure is split into multiple subsets named spatial window substructures Figure 4.

A distinctive feature of our model, in contrast to GCNs, is the partitioning of the keypoint graph into spatial windows rather than utilizing the entire graph as input. In

the single-view pose estimation methods, inconsistencies in keypoint generation are omnipresent, especially for hand keypoints. These discrepancies often arise from factors such as motion blur, occlusion by body parts, and low video resolution, leading to misplacement of hand keypoints. To mitigate these issues we divide the whole graph into multiple spatial windows by stacking the part keypoints combinations. This spatial division restricts the flow of information from one window to another. With this approach, for one-handed signs, a window only contains the signing hand, thereby eliminating the potential influence of the non-signing hand's motion. The creation of these spatial windows is formalized as follows:

For each frame, the input keypoints  $K = 27$  are divided into 5 spatial subsets corresponding to body parts: *face*, *left*

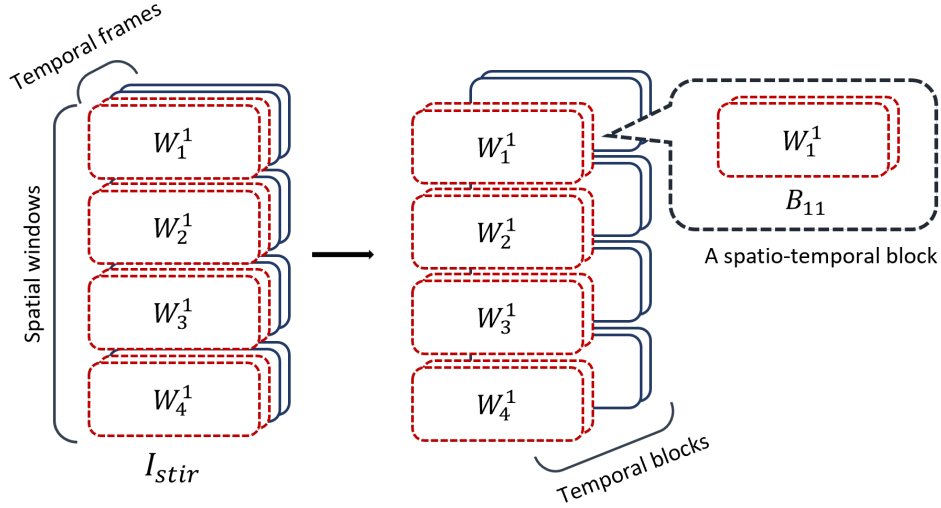


Figure 7. The temporal frames are divided into temporal blocks where each temporal block contains multiple frames. Each spatial window with its respective temporal block creates a spatio-temporal block.

*arm, left hand, right arm, and right hand*, as illustrated in the Figure 4. For a spatial window  $j$  in frame  $f$ , the stack of face (3 keypoints), any one arm (3 keypoints) and any one hand (10 keypoints) are taken to obtain  $W_j^f$  keypoints subset with  $w_k = 16$  keypoints. If there are  $S$  spatial windows per frame then they are stacked to generate the output frame with  $K' = S \times w_k$  keypoints. For a skeleton input sign video  $I \in \mathbb{R}^{F \times K \times d}$  with  $F$  frames and  $K$  keypoints per frame in  $d (= 2)$  dimensions, output  $I' \in \mathbb{R}^{F \times K' \times d}$  is our spatial window representation.

It was demonstrated that the Fourier feature mapping allows a model to learn high-frequency functions more effectively [47]. This process involves embedding the low-dimensional input coordinates into a higher-dimensional space. Specifically, our low  $d$  dimensional node input representation is embedded into a higher dimension  $d'$  using the Fourier feature mapping. Finally, we get our spatio-temporal input representation  $I_{stir} \in \mathbb{R}^{F \times K' \times d'}$ .

We incorporated the frame position as a sequential marker into the input embeddings using a fixed positional encoding scheme similar to the one proposed by Vaswani *et al.* [49].

## 4.2. Part Attention Layer

The individual signs depend on the motion of different parts and we want to capture that using spatio-temporal part attention layer. To learn different part attention, we design a part attention layer consisting of *two* key components: *part attention block*, and *temporal merge* shown in Figure 3.

### 4.2.1 Part Attention Block

The part attention block is the fundamental component of each part attention layer. The different contextual features are accumulated through information propagation between nodes by utilizing multiple part attention blocks within each part attention layer. The part attention block has *three* key components, *temporal blocks*, *temporal shift*, and *graph attention block* shown in Figure 3.

**Temporal Blocks:** Temporally consecutive frames tend to have very subtle changes in spatial graphs, and these changes can be effectively captured by grouping frames within a block. This grouping approach is inspired by the hierarchical divide-and-conquer paradigm. The attention mechanism is applied within these blocks to capture local context and focus on granular movement changes. Subsequently, these blocks are merged to capture the entire temporal context. To implement this, the embedded spatio-temporal input representation  $I_{stir}$  (input sequence) is divided into multiple temporal blocks, each consisting of consecutive frames. Let each temporal block contain  $T$  consecutive frames which divide  $F$  temporal frames into  $F'$  consecutive blocks such that  $F = F' \times T$ . Let  $B_{ij} \in \mathbb{R}^{T \times K' \times d'}$  be the spatio-temporal block consists of  $i^{th}$  spatial window and  $j^{th}$  temporal block shown in Figure 7.

**Temporal Shift:** In our proposed network, the restriction of attention within each spatio-temporal block limits the sharing of information between consecutive temporal blocks. To address this issue, we have used a shifting mechanism inspired by [27] that shifts the



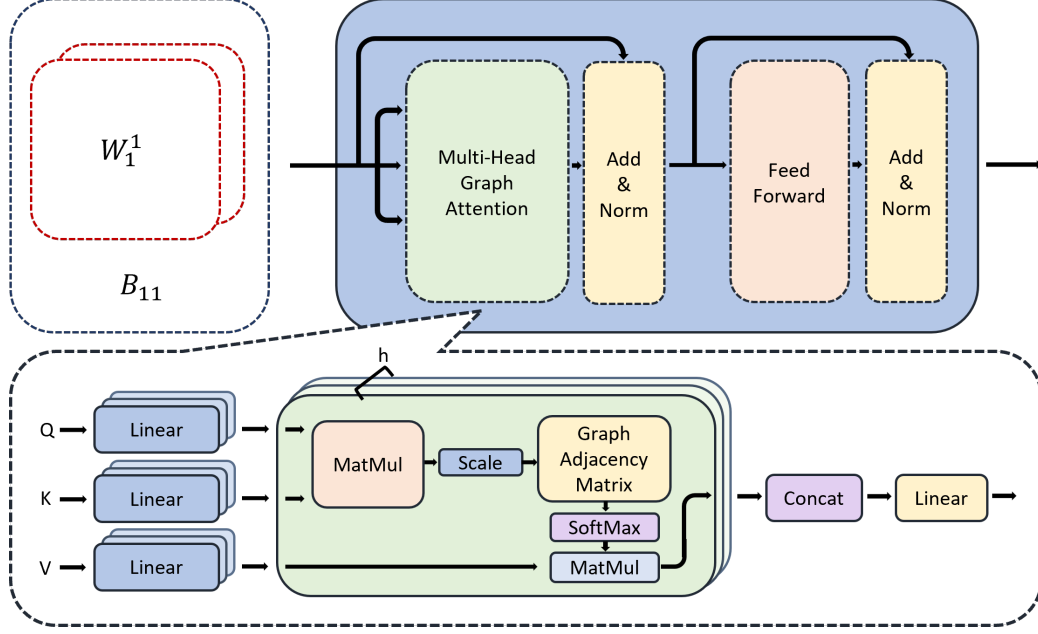


Figure 8. The Graph Attention Block consists of the multi-head graph attention module along with normalization and feed-forward layers. The multi-head graph attention module with scaled dot product graph attention is the basic attention block which uses the graph adjacency matrix.

temporal window through the input sequence resulting in the propagation of information between consecutive temporal blocks. In this mechanism, frames that fall outside the first window are rolled and appended at the end of the temporal sequence. These rolled frames are masked during attention operation to ensure they do not influence the graph attention values in the last temporal block. Let  $f_i \in \mathbb{R}^{K' \times d'}$  be the  $i^{th}$  frame of our spatio-temporal input representation  $I_{stir} = \{f_1, f_2, \dots, f_F\}$ . Then after  $s$  shift we get  $I_{stir}^s = \{f_{s+1}, f_{s+2}, \dots, f_F, f_1, f_2, \dots, f_s\}$ .

### Graph Attention Block:

The graph attention block, illustrated in Figure 8, is designed to operate on spatio-temporal block  $B_{ij}$ . This module accumulates information from the neighboring nodes using the attention mechanism that utilizes node feature similarity, rather than using a convolution kernel. To preserve our skeleton structure the attention mechanism is restricted to the neighboring nodes connected by edges and belong to the same spatio-temporal block. We used an attention mask called edge bias following the human joint-bone connectivity as an inductive bias to restrict the attention mechanism. We followed the spatio-temporal edge connectivity described in the input representation Section 4.1. In every spatio-temporal block  $B_{ij}$  for  $i^{th}$  spatial window and  $j^{th}$  temporal block, the connectivity is further restricted according to the corresponding edge set  $e_{pq} \in E(G)$ . The edge set  $e_{pq}$  is used to create a Graph Adjacency Matrix

$A_{pq}$  for the spatio-temporal block  $B_{ij}$ .

Let  $n$  be the total number of keypoints within the  $(i, j)^{th}$  spatio-temporal block, then  $B_{ij} \in \mathbb{R}^{n \times d'}$  such that  $n = T \times K'$ . We define our graph attention ( $GAttn$ ) and other modules shown in Figure 8 as:

$$\begin{aligned}
 GAttn &= \text{Softmax}\left(\frac{QK^T}{\sqrt{h}} \odot A_{pq}\right) \\
 Q &= \text{Norm}(B_{ij}) \times W^q \\
 K &= \text{Norm}(B_{ij}) \times W^k \\
 V &= \text{Norm}(B_{ij}) \times W^v \\
 B'_{ij} &= B_{ij} + GAttn \times V \\
 O_{ij} &= B'_{ij} + FF(\text{Norm}(B'_{ij}))
 \end{aligned} \tag{2}$$

where  $W^q, W^k, W^v$  are the model parameters similar to the multi head attention in [49] and  $\odot, \times$  represent the element-wise multiplication and matrix multiplication respectively. Here we use *layer normalization* as  $Norm$  to normalize the input,  $FF$  is a feed-forward layer, and the output  $O_{ij}$  represents the embedding of  $B_{ij}$  which exhibits the local spatio-temporal contextual information.

Through our observations, we found that the attention weights given to similar adjacent nodes are high due to their feature similarity (eg. nose keypoint along temporal connections in edge connectivity defined in (1)). The high attention values among similar nodes can sometimes reduce

the attention weights of other nodes, leading to a loss of important information. To overcome this issue, we propose an attention dropout mechanism inspired by [53]. But, instead of randomly nullifying attention weights, our proposed regularization technique is more likely to drop attention between two nodes with higher attention value. First a random variable  $\gamma$  is uniformly sampled from  $(0, 1)$ . Then the attention matrix  $GAttn$  is masked with value 0 where  $GAttn$  is greater than  $\gamma$ .

#### 4.2.2 Temporal Merge

The attention mechanism in the first *Part Attention Layer* captures the local spatio-temporal features. To obtain global context, we use a hierarchical temporal merging technique. In each *Part Attention Layer*, following the  $M$  graph attention operations, the number of temporal frames is reduced by merging frames within each temporal block, resulting in upper-level contextual attention in deeper *Part Attention Layers*. For a spatio-temporal input  $I_{stir} \in \mathbb{R}^{F \times K' \times d'}$  and temporal block size  $T$ , after first merging we get a spatio-temporal contextual embedding in  $\mathbb{R}^{(F/T) \times K' \times (d' \times T)}$ .

After  $N$  *Part Attention Layer* we use an average pooling over all the spatial windows to represent the final spatio-temporal contextual embedding. Finally, a fully connected layer utilizes this embedded feature to classify each sign.

### 5. Experimental Evaluation

In this section, first, we evaluate our proposed dataset compared to other existing isolated Indian sign language datasets. Then we evaluated our proposed model in isolated ISL datasets as well as in other isolated SL datasets. We conducted extensive ablation studies to evaluate the effectiveness of various design choices of our model development. Here we start with a brief description of all the datasets used in our experiment, then experimental settings, and data pre-processing followed by discussions of all the results.

#### 5.1. Datasets

To evaluate our proposed FDMSE-ISL dataset, we considered a state-of-the-art ISL dataset called INCLUDE [46]. It contains a vocabulary size of 262 words with 4285 video samples in  $1920 \times 1080$  resolution. This dataset is created in lab settings and has imbalanced samples in classes. A detailed description of the FDMSE-ISL dataset is presented in Section 3.

In addition to our dataset and INCLUDE, we evaluated our proposed model on 3 other isolated SL datasets namely AUTSL [45], LSA64 [41] and WLASL [25]. The WLASL [25] is an isolated American sign language dataset with 2000 glosses and 21083 samples. The videos were

collected from web sources and were recorded in unconstrained real-life settings. AUTSL [45] is a Turkish sign language dataset comprising 38336 samples throughout 226 glosses. The videos are recorded in real-life conditions with multiple backgrounds. LSA64 [41] is an Argentinian sign language dataset having 3200 videos over 64 signs. The videos were recorded in lab settings with static backgrounds.

For all the datasets we follow the author-given data partitions for all the evaluations. Since there was no validation set available in the INCLUDE dataset we made a validation set which contains 10% data from the train set.

For our extensive ablation study, we considered a 20% subset of our proposed dataset due to our experimental resource limitations. We call this subset as FDMSE-ISL400. It contains 400 classes with 8000 video samples and these 400 classes were chosen from 2002 classes with Simple Random Sampling without replacement (SRSWOR) sampling procedure and tried to preserve the frame statistics. A comparison (with respect to the number of signs, number of videos, number of unique signers, video source, and total duration) of all these datasets summary is shown in Table 1 and frame statistics are in Table 3.

#### 5.2. Experimental Settings

In the keypoint based approaches, first, we have to detect the body keypoints effectively. There are many keypoints detection or pose estimation methods available in the literature, some notables are OpenPose [7], MediaPipe holistic [29], HR-net [51], and others [36, 40, 55]. Here we have considered MediaPipe holistic [29] for our pose estimations due to its balance in both accuracy and processing speed compared to others. The MediaPipe holistic gives a total of 543, 3D keypoints (468 for face, 33 for pose, and 21 per hand) per video frame. Out of these, we considered 27 keypoints (3 facial keypoints (nose, 2 eyes), 2 shoulders, 2 elbows, and 10 keypoints from each hand) with  $x$  and  $y$  coordinates for our skeleton representation.

We implemented all the models in Python<sup>2</sup> using the PyTorch toolbox<sup>3</sup> and trained on a system running on Ubuntu 22.04 OS, 192 GB RAM, Xeon gold 32-core CPU and NVIDIA A100 80G GPU. To train the models AdamW Optimizer was used with an initial learning rate of  $1e^{-4}$  with the Cosine Annealing scheduler having a patience of 20 epochs. The max training epochs were set to 4000 with early stopping on validation loss, set to the patience of 400 epochs. The objective function used for training is label smoothed cross entropy loss [13]. For all our experiments, we report top-1 and top-5 per instance accuracy as the performance measure.

<sup>2</sup><https://www.python.org/>

<sup>3</sup><https://pytorch.org/>

Table 3. Comparison of dataset frame statistics.

Frame Statistics	FDMSE-ISL	FDMSE-ISL400	WLASL	AUTSL	LSA64	INCLUDE
# Videos	40033	8000	21095	36302	3200	4284
Mean	195.40	195.07	60.55	60.97	82.75	64.27
Standard Deviation	40.04	39.98	23.56	10.96	27.58	14.96
Minimum	30.00	90.00	9.00	7.00	14.00	33.00
1st Quartile	180.00	180.00	43.00	54.00	65.00	54.00
Median	180.00	180.00	58.00	60.00	78.00	62.00
3rd Quartile	210.00	210.00	74.00	67.00	100.00	71.25
Maximum	570.00	570.00	282.00	156.00	201.00	154.00

### 5.3. Data Pre-processing and Augmentations

Various data pre-processing techniques are used to normalize the data and data augmentation techniques are employed during training to increase the model robustness.

Instead of the normalized coordinates of the keypoints generated by the Mediapipe holistic  $([0, 1])$ , we used the keypoint coordinates with respect to the image size by multiplying the height and width (frame size) of the sign video.

In real-life video recording scenarios, subjects can appear anywhere within the image plane and with different scales. We normalise the keypoint coordinates to achieve location and scale invariance for keypoints using dynamic bounding boxes. Additionally, we apply shear and rotation transformations during training to the keypoints to introduce subtle random variations, inspired by [44].

After using mediapipe holistic we observed occasional failures in detecting hand keypoints. Instead of seeing this as a limitation, we integrated this occurrence into our framework by intentionally masking hand keypoints in certain frames. We sample some frames with hyperparameter sampling probability  $\beta$  following the SRSWOR sampling procedure and mask all the hand keypoints. Next, these frames are filled with approximated hand keypoints using spherical linear interpolation technique. This missing data-filling technique ensures a stable learning process for our graph networks.

According to the ISL experts, signing speed differs from signer to signer. To incorporate this speed variability we introduce the temporal augmentation technique by randomly reducing or increasing the number of frames through SR-SWOR or Simple Random Sampling with replacement (SR-SWR) sampling procedure.

The video clips can have any number of frames while the models require a fixed number of frames. To combat this inconsistent number of frames, temporal sampling is introduced. If a video clip contains fewer frames than needed, we pad it with a random offset at the beginning and accordingly adjust at the end. Conversely, if the video contains more frames than required, we uniformly sample the necessary number of frames from the clip.

### 5.4. Results

#### 5.4.1 Ablation Study

We have conducted an ablation study for different hyperparameters (*number of spatial windows, temporal blocks, temporal shift, edge bias, regularizer*) of our proposed HW-GAT model. For this study, we have used a subset called FDMSE-ISL400 of our proposed dataset and report top-1 and top-5 per instance accuracy as performance measurements.

**Number of spatial windows:** The division of each skeleton frame into spatial windows is a distinctive feature of our proposed model’s input representation. We have experimented with *three* different numbers of spatial windows (1, 2, 4) defined as follows:

- In the case of 1 spatial window, there is no division of the skeleton spatial structure.
- For 2 spatial window, we divide the skeleton spatial structure into 2 substructures: *substructure-1* (contains head, left arm, and left hand) and *substructure-2* (contains head, right arm, and right hand).
- In the case of 4 spatial window, we divide the skeleton spatial structure into 4 substructures: *substructure-1* (contains head, left arm, and left hand), *substructure-2* (contains head, left arm, and right hand), *substructure-3* (contains head, right arm, and left hand) and *substructure-4* (contains head, right arm, and right hand).

The results of these *three* spatial windows divisions are shown in Table 4 and the 4 spatial windows give the highest performance of top-1 95.94% and top-5 99.44% accuracy. Also, these results indicate that the proposed substructure-based model performs relatively better than the whole graph input representation (1 spatial window).

**Temporal block length:** The accuracy reaches the top when the temporal block length is set to 2 as demonstrated in Table 5. The temporal block length being 2 enforces



Figure 9. Inter class similarity in signs "Low" vs. "Short/Young" and "Seat" vs. "Bench".

Table 4. Impact of number of spatial windows on FDMSE-ISL400 dataset.

# Spatial Windows	Test Accuracy	
	Top-1	Top-5
1	95.37	99.22
2	94.59	99.22
4	<b>95.94</b>	<b>99.44</b>

Table 5. Impact of length of temporal blocks on FDMSE-ISL400 dataset.

Temporal Block Length	Test Accuracy	
	Top-1	Top-5
2	<b>95.94</b>	<b>99.44</b>
4	94.97	99.31

Table 6. Impact of temporal shift on FDMSE-ISL400 dataset.

Shifting Window	Test Accuracy	
	Top-1	Top-5
Without Shift	94.97	99.31
With Shift	<b>95.94</b>	<b>99.44</b>

Table 7. Impact of edge bias on FDMSE-ISL400 dataset.

Edge Bias Type	Test Accuracy	
	Top-1	Top-5
Learnable Edge Bias	95.53	99.41
Without Edge Bias	95.16	99.00
With Edge Bias	<b>95.94</b>	<b>99.44</b>

Table 8. Impact of regularizer on FDMSE-ISL400 dataset.

Presence of Regularizer	Test Accuracy	
	Top-1	Top-5
No Regularizer	95.94	99.44
Regularizer	<b>96.63</b>	<b>99.47</b>

the model to capture the temporal dynamics in consecutive frames.

**Effect of temporal shift:** Table 6 shows the results of

the temporal shift mechanism as described in Section 4.2.1. The temporal window shifting allows the information propagation between consecutive temporal blocks resulting in better top-1 and top-5 accuracy compared to without shifting.

**Effect of edge bias:** The proposed edge bias described in Section 4.2.1 has a relatively better impact on the final classification task as shown in Table 7. Our proposed edge bias gives 0.78 percentage points top-1 accuracy compared to the without edge bias mainly due to the attention mechanism being restricted to each spatio-temporal block according to the skeleton structure.

**Impact of regularizer:** The proposed attention dropout regularization technique described in Section 4.2.1 gives better performance (0.69 percentage point in top-1 and 0.03 percentage point in top-5) compared to without regularizer.

## 5.4.2 Evaluation of proposed dataset

To evaluate our proposed dataset, we consider our proposed model, a baseline transformer-based model, and *two* state-of-the-art skeleton-based models ST-GCN [18] and SL-GCN [18]. We compared the results with an isolated ISL dataset INCLUDE [46]. Table 9 shows the top-1 and top-5 performance of all the methods on the proposed and INCLUDE datasets. From Table 9 we see that on the proposed dataset all the models perform less compared to the INCLUDE datasets. This surmise that the proposed dataset is more challenging, may be due to higher number of classes and atomic signs being the subsets of composite signs classes. Also, there is a lot of inter-class similarity between two different signs like 'Low' Vs. 'Short/Young', 'Seat' Vs. 'Bench' etc. shown in Figure 9. To see the effect of knowledge transfer, we pre-trained our proposed model on the proposed dataset and fine-tuned (200 epochs) it on the INCLUDE dataset. We achieved top-1 with 97.79% and top-5 with 99.26% as shown in the last row of Table 9. This result shows the utility of the proposed dataset for the ISL recognition task as a pre-training dataset on relatively smaller isolated ISL datasets similar to INCLUDE.

Table 9. Comparing of results for Indian sign language dataset.

Method	INCLUDE		FDMSE-ISL	
	Top-1	Top-5	Top-1	Top-5
Transformer	94.85	99.14	89.71	97.95
ST-GCN [44]	96.69	99.14	93.57	99.01
SL-GCN [44]	96.57	<b>99.26</b>	93.39	98.98
HWGAT	97.67	<b>99.26</b>	<b>93.86</b>	<b>99.19</b>
HWGAT (Finetuned)	<b>97.79</b>	<b>99.26</b>	-	-

Table 10. Comparison of results for other sign language datasets.

Methods	LSA64		AUTSL		WLASL	
	Top-1	Top-5	Top-1	Top-5	Top-1	Top-5
Pose-GRU [25]	-	-	-	-	22.54	49.81
Pose-TGCN [25]	-	-	-	-	23.65	51.75
Transformer	90.00	98.12	90.19	98.61	23.20	-
ST-GCN [44]	92.81	98.43	90.67	98.66	34.40	66.57
SL-GCN [18]	98.13	<b>100.00</b>	95.02	-	41.65	74.68
HWGAT	97.81	99.84	95.43	99.17	43.28	74.92
HWGAT (Finetuned)	<b>98.59</b>	99.84	<b>95.80</b>	<b>99.49</b>	<b>48.49</b>	<b>80.86</b>

### 5.4.3 Evaluation of proposed model

To evaluate the proposed model, we used our proposed dataset as well as four other SL datasets: INCLUDE (Indian sign language), LSA64 (Argentinian sign language), AUTSL (Turkish sign language), and WLASL (American sign language) as described in Section 5.1. Table 9 summarizes a comparative analysis with state-of-the-art skeleton-based models on ISL datasets, highlighting that our proposed model either performs better or exhibits similar results compared to other models. Table 10 demonstrates the ability of the proposed model across different other sign language datasets. The proposed model achieves the highest performance in both top-1 (95.43%, 43.28%) and top-5 (99.17%, 74.92%) for AUTSL and WLASL respectively. For the LSA64 dataset, the proposed model gives comparable results in both top-1 and top-5 performance measure. When we fine-tune (pre-trained on the proposed dataset) our model, we achieve the highest top-1 performance for all the datasets as shown in the last row of Table 10.

## 6. Conclusion

In conclusion, we presented a new large-scale isolated Indian sign language dataset and a novel sign language recognition model based on the skeleton graph structure. The proposed dataset is not only large-scale but also contains characteristics such as gender-balanced, class-balanced, multi-modal and multi-view. The proposed model tries to capture the distinctive characteristics of different signs by restricting the attention between interacting body parts in the skeleton graph structure. Compar-

ative analysis of the proposed dataset with the state-of-the-art isolated ISL dataset using different state-of-the-art skeleton-based models shows the importance of our proposed dataset. The proposed model has been evaluated on different sign language (Indian, American, Argentinian, and Turkish) datasets giving better or comparable results against the state-of-the-art skeleton-based models. Also, the utility of the proposed dataset is shown by the knowledge transfer (or fine-tuning) experiment using the proposed model throughout different sign language datasets. We believe that the proposed dataset (with different modalities) will accelerate the ISL recognition task and be useful for other SL recognition tasks. In addition, other multiview modalities would be useful for keypoints correction, pose estimation, 3D-model generation, general gesture recognition and other related tasks. Furthermore, our word grouping based on the number of glosses can be used in classrooms for regular ISL teaching and learning purposes.

## Acknowledgement

This work is partially funded by VECC, Kolkata. We thank Mr. Subhankar Nag for the data processing and model discussions.

## References

- [1] Nikolas Adaloglou, Theocharis Chatzis, Ilias Papastratis, Andreas Stergioulas, Georgios Th. Papadopoulos, Vassia Zacharopoulou, George J. Xydopoulos, Klimnis Atzakis, Dimitris Papazachariou, and Petros Daras. A comprehen-

- sive study on deep learning-based methods for sign language recognition, 2021. 1, 3
- [2] S Ajay, Ajith Potluri, Sara Mohan George, R Gaurav, and S Anusri. Indian sign language recognition using random forest classifier. In *2021 IEEE International Conference on Electronics, Computing and Communication Technologies (CONECCT)*, pages 1–6. IEEE, 2021. 3
- [3] Samuel Albanie, Gül Varol, Liliane Momeni, Hannah Bull, Triantafyllos Afouras, Himel Chowdhury, Neil Fox, Bencie Woll, Rob Cooper, Andrew McParland, et al. Bbc-oxford british sign language dataset. *arXiv preprint arXiv:2111.03635*, 2021. 2
- [4] Vassilis Athitsos, Carol Neidle, Stan Sclaroff, Joan Nash, Alexandra Stefan, Quan Yuan, and Ashwin Thangali. The american sign language lexicon video dataset. In *2008 IEEE Computer Society Conference on Computer Vision and Pattern Recognition Workshops*, pages 1–8. IEEE, 2008. 1, 3
- [5] Matyáš Boháček and Marek Hruží. Sign pose-based transformer for word-level sign language recognition. In *Proceedings of the IEEE/CVF Winter Conference on Applications of Computer Vision*, pages 182–191, 2022. 4
- [6] Necati Cihan Camgoz, Oscar Koller, Simon Hadfield, and Richard Bowden. Sign language transformers: Joint end-to-end sign language recognition and translation. In *IEEE Conference on Computer Vision and Pattern Recognition (CVPR)*, 2020. 4
- [7] Zhe Cao, Tomas Simon, Shih-En Wei, and Yaser Sheikh. Realtime multi-person 2d pose estimation using part affinity fields. In *Proceedings of the IEEE conference on computer vision and pattern recognition*, pages 7291–7299, 2017. 4, 10
- [8] MMPose Contributors. Openmmlab pose estimation toolbox and benchmark. <https://github.com/open-mmlab/mmpose>, 2020. 4
- [9] Navneet Dalal and Bill Triggs. Histograms of oriented gradients for human detection. In *2005 IEEE computer society conference on computer vision and pattern recognition (CVPR'05)*, volume 1, pages 886–893. Ieee, 2005. 3
- [10] Soumen Das, Saroj Kr. Biswas, and Biswajit Purkayastha. Occlusion robust sign language recognition system for indian sign language using cnn and pose features. *Multimedia Tools and Applications*, 2024. 3
- [11] Deafness and hearing loss. <https://www.who.int/news-room/fact-sheets/detail/deafness-and-hearing-loss>. Accessed: 2024-04-10. 1
- [12] Sarah Ebling, Necati Cihan Camgöz, Penny Boyes Braem, Katja Tissi, Sandra Sidler-Miserez, Stephanie Stoll, Simon Hadfield, Tobias Haug, Richard Bowden, Sandrine Tornay, et al. Smile swiss german sign language dataset. In *Proceedings of the 11th International Conference on Language Resources and Evaluation (LREC) 2018*. The European Language Resources Association (ELRA), 2018. 3
- [13] Tong He, Zhi Zhang, Hang Zhang, Zhongyue Zhang, Junyuan Xie, and Mu Li. Bag of tricks for image classification with convolutional neural networks. In *2019 IEEE/CVF Conference on Computer Vision and Pattern Recognition (CVPR)*, pages 558–567, 2019. 10
- [14] Berthold KP Horn and Brian G Schunck. Determining optical flow. *Artificial intelligence*, 17(1-3):185–203, 1981. 3
- [15] Jie Huang, Wengang Zhou, Qilin Zhang, Houqiang Li, and Weiping Li. Video-based sign language recognition without temporal segmentation. In *Proceedings of the AAAI Conference on Artificial Intelligence*, volume 32, 2018. 3
- [16] Indian sign language dictionary. <https://indiansignlanguage.org/>. Accessed: 2024-04-10. 4
- [17] Songyao Jiang, Bin Sun, Lichen Wang, Yue Bai, Kunpeng Li, and Yun Fu. Sign language recognition via skeleton-aware multi-model ensemble. *arXiv preprint arXiv:2110.06161*, 2021. 3, 4, 6
- [18] Songyao Jiang, Bin Sun, Lichen Wang, Yue Bai, Kunpeng Li, and Yun Fu. Skeleton aware multi-modal sign language recognition. In *Proceedings of the IEEE/CVF Conference on Computer Vision and Pattern Recognition*, pages 3413–3423, 2021. 3, 6, 12, 13
- [19] Abhinav Joshi, Ashwani Bhat, Pradeep S, Priya Gole, Shashwat Gupta, Shreyansh Agarwal, and Ashutosh Modi. CISLR: Corpus for Indian Sign Language recognition. In *Proceedings of the 2022 Conference on Empirical Methods in Natural Language Processing*, pages 10357–10366. Association for Computational Linguistics, 2022. 2, 3
- [20] Hamid Reza Vaezi Joze and Oscar Koller. Ms-asl: A large-scale data set and benchmark for understanding american sign language. *arXiv preprint arXiv:1812.01053*, 2018. 1, 3
- [21] G. Khartheesvar, Mohit Kumar, Arun Kumar Yadav, and Divakar Yadav. Automatic indian sign language recognition using mediapipe holistic and lstm network. *Multimedia Tools and Applications*, 2023. 4
- [22] P.V.V. Kishore and Panakala rajesh kumar. A video based indian sign language recognition system (inslr) using wavelet transform and fuzzy logic. *International Journal of Engineering and Technology*, 4:537–542, 01 2012. 2
- [23] Oscar Koller, Hermann Ney, and Richard Bowden. Deep hand: How to train a cnn on 1 million hand images when your data is continuous and weakly labelled. In *Proceedings of the IEEE conference on computer vision and pattern recognition*, pages 3793–3802, 2016. 3
- [24] Oscar Koller, O Zargaran, Hermann Ney, and Richard Bowden. Deep sign: Hybrid cnn-hmm for continuous sign language recognition. In *Proceedings of the British Machine Vision Conference 2016*, 2016. 3
- [25] Dongxu Li, Cristian Rodriguez, Xin Yu, and Hongdong Li. Word-level deep sign language recognition from video: A new large-scale dataset and methods comparison. In *Proceedings of the IEEE/CVF winter conference on applications of computer vision*, pages 1459–1469, 2020. 1, 3, 4, 10, 13
- [26] Tao Liu, Wengang Zhou, and Houqiang Li. Sign language recognition with long short-term memory. In *2016 IEEE international conference on image processing (ICIP)*, pages 2871–2875. IEEE, 2016. 1, 3, 4
- [27] Ze Liu, Yutong Lin, Yue Cao, Han Hu, Yixuan Wei, Zheng Zhang, Stephen Lin, and Baining Guo. Swin transformer: Hierarchical vision transformer using shifted windows, 2021. 8

- [28] David G Lowe. Distinctive image features from scale-invariant keypoints. *International journal of computer vision*, 60:91–110, 2004. 3
- [29] Camillo Lugaresi, Jiuqiang Tang, Hadon Nash, Chris McClanahan, Esha Uboweja, Michael Hays, Fan Zhang, Chuoling Chang, Ming Guang Yong, Juhyun Lee, Wan-Teh Chang, Wei Hua, Manfred Georg, and Matthias Grundmann. Mediapipe: A framework for building perception pipelines, 2019. 4, 10
- [30] Debapriya Maji, Soyeb Nagori, Manu Mathew, and Deepak Poddar. Yolo-pose: Enhancing yolo for multi person pose estimation using object keypoint similarity loss. In *Proceedings of the IEEE/CVF Conference on Computer Vision and Pattern Recognition*, pages 2637–2646, 2022. 4
- [31] Liliame Momeni, Gul Varol, Samuel Albanie, Triantafyllos Afouras, and Andrew Zisserman. Watch, read and lookup: learning to spot signs from multiple supervisors. In *Proceedings of the Asian Conference on Computer Vision*, 2020. 2, 3
- [32] Anup Nandy, Jay Shankar Prasad, Soumik Mondal, Pavan Chakraborty, and G. C. Nandi. Recognition of isolated indian sign language gesture in real time. In *Information Processing and Management*, pages 102–107, Berlin, Heidelberg, 2010. Springer Berlin Heidelberg. 2
- [33] Oğulcan Özdemir and Kindiroğlu. Bosphorussign22k sign language recognition dataset. *arXiv preprint arXiv:2004.01283*, 2020. 3
- [34] Ronald Poppe. Poppe, r.: A survey on vision-based human action recognition. *image and vision computing* 28(6), 976–990. *Image Vision Comput.*, 28:976–990, 06 2010. 2
- [35] Lawrence Rabiner and Biinghwang Juang. An introduction to hidden markov models. *ieee assp magazine*, 3(1):4–16, 1986. 3
- [36] Umer Rafi, Bastian Leibe, Juergen Gall, and Ilya Kostrikov. An efficient convolutional network for human pose estimation. In *BMVC*, volume 1, page 2, 2016. 10
- [37] JL Raheja, Anand Mishra, and Ankit Chaudhary. Indian sign language recognition using svm. *Pattern Recognition and Image Analysis*, 26:434–441, 2016. 3
- [38] G. Anantha Rao, K. Syamala, P. V. V. Kishore, and A. S. C. S. Sastry. Deep convolutional neural networks for sign language recognition. In *2018 Conference on Signal Processing And Communication Engineering Systems (SPACES)*, pages 194–197, 2018. 3
- [39] J. Rekha, J. Bhattacharya, and S. Majumder. Shape, texture and local movement hand gesture features for indian sign language recognition. In *3rd International Conference on Trendz in Information Sciences & Computing (TISC2011)*, pages 30–35, 2011. 2
- [40] Pengfei Ren, Haifeng Sun, Qi Qi, Jingyu Wang, and Weiting Huang. Srn: Stacked regression network for real-time 3d hand pose estimation. In *BMVC*, page 112, 2019. 10
- [41] Franco Ronchetti, Facundo Quiroga, Cesar Estrebow, Laura Lanzarini, and Alejandro Rosete. Lsa64: A dataset of argentinian sign language. *XX II Congreso Argentino de Ciencias de la Computación (CACIC)*, 2016. 1, 2, 3, 10
- [42] Wendy Sandler and Diane Lillo-Martin. *Sign Language and Linguistic Universals*. Cambridge University Press, Cambridge, United Kingdom, 2006. 1
- [43] Zed Sevcikova Sehyr, Naomi Caselli, Ariel M Cohen-Goldberg, and Karen Emmorey. The asl-lex 2.0 project: A database of lexical and phonological properties for 2,723 signs in american sign language. *The Journal of Deaf Studies and Deaf Education*, 26(2):263–277, 2021. 3
- [44] Prem Selvaraj, Gokul NC, Pratyush Kumar, and Mitesh Khapra. Openhands: Making sign language recognition accessible with pose-based pretrained models across languages, 2021. 4, 6, 11, 13
- [45] Ozge Mercanoglu Sincan and Hacer Yalim Keles. Autsl: A large scale multi-modal turkish sign language dataset and baseline methods. *IEEE Access*, 8:181340–181355, 2020. 1, 2, 3, 10
- [46] Advait Sridhar, Rohith Gandhi Ganesan, Pratyush Kumar, and Mitesh Khapra. Include: A large scale dataset for indian sign language recognition. In *Proceedings of the 28th ACM international conference on multimedia*, pages 1366–1375, 2020. 1, 2, 3, 5, 10, 12
- [47] Matthew Tancik, Pratul P. Srinivasan, Ben Mildenhall, Sara Fridovich-Keil, Nithin Raghavan, Utkarsh Singhal, Ravi Ramamoorthi, Jonathan T. Barron, and Ren Ng. Fourier features let networks learn high frequency functions in low dimensional domains. In *Proceedings of the 34th International Conference on Neural Information Processing Systems, NIPS '20*, Red Hook, NY, USA, 2020. Curran Associates Inc. 8
- [48] Alaa Tharwat, Tarek Gaber, Aboul Ella Hassanien, Mohamed K Shahin, and Basma Refaat. Sift-based arabic sign language recognition system. In *Afro-European Conference for Industrial Advancement: Proceedings of the First International Afro-European Conference for Industrial Advancement AECIA 2014*, pages 359–370. Springer, 2015. 1, 3
- [49] Ashish Vaswani, Noam Shazeer, Niki Parmar, Jakob Uszkoreit, Llion Jones, Aidan N Gomez, Łukasz Kaiser, and Illia Polosukhin. Attention is all you need. *Advances in neural information processing systems*, 30, 2017. 2, 8, 9
- [50] Hanjie Wang, Xiujuan Chai, Xiaopeng Hong, Guoying Zhao, and Xilin Chen. Isolated sign language recognition with grassmann covariance matrices. *ACM Transactions on Accessible Computing (TACCESS)*, 8(4):1–21, 2016. 3
- [51] Jingdong Wang, Ke Sun, Tianheng Cheng, Borui Jiang, Chaorui Deng, Yang Zhao, Dong Liu, Yadong Mu, Mingkui Tan, Xinggang Wang, et al. Deep high-resolution representation learning for visual recognition. *IEEE transactions on pattern analysis and machine intelligence*, 43(10):3349–3364, 2020. 10
- [52] Sijie Yan, Yuanjun Xiong, and Dahua Lin. Spatial temporal graph convolutional networks for skeleton-based action recognition. In *Proceedings of the AAAI conference on artificial intelligence*, volume 32, 2018. 4, 6
- [53] Lin Zehui, Pengfei Liu, Luyao Huang, Junkun Chen, Xipeng Qiu, and Xuanjing Huang. Dropattention: A regularization method for fully-connected self-attention networks, 2019. 10
- [54] Jihai Zhang, Wengang Zhou, Chao Xie, Junfu Pu, and Houqiang Li. Chinese sign language recognition with adap-

- tive hmm. In *2016 IEEE international conference on multimedia and expo (ICME)*, pages 1–6. IEEE, 2016. [1](#), [2](#), [3](#)
- [55] Zhiming Zou, Kenkun Liu, Le Wang 0003, and Wei Tang. High-order graph convolutional networks for 3d human pose estimation. In *BMVC*, 2020. [10](#)
- [56] Ronglai Zuo, Fangyun Wei, and Brian Mak. Natural language-assisted sign language recognition, 2023. [4](#)